Design of an Active Noise Reduction System for a Cogeneration Plant

Emanuele Voltolini
Dept. of Engineering and Architecture
University of Parma
Parma, Italy
emanuele.voltolini@unipr.it

Daniel Pinardi
Dept. of Engineering and Architecture
University of Parma
Parma, Italy
daniel.pinardi@unipr.it

Andrea Toscani
Dept. of Engineering and Architecture
University of Parma
Parma, Italy
andrea.toscani@unipr.it

Marco Binelli
Dept. of Engineering and Architecture
University of Parma
Parma, Italy
marco.binelli@unipr.it

Angelo Farina
Dept. of Engineering and Architecture
University of Parma
Parma, Italy
angelo.farina@unipr.it

Jessica Ferrari
Dept. of Engineering and Architecture
University of Parma
Parma, Italy
jessica.ferrari@unipr.it

Stefano Maglia
AB Impianti Srl
Brescia, Italy
stefano.maglia@gruppoab.it

Andrea Zenaro
AB Impianti Srl
Brescia, Italy
andrea.zenaro@gruppoab.it

Enrico Calzavacca
AB Impianti Srl
Brescia, Italy
enrico.calzavacca@gruppoab.it

***Abstract*—Active noise control (ANC) aims at reducing the amplitude of a primary sound source by emitting a controlling sound wave through one or more devices, so that the two waves sum out of phase at the listening point. To generate such out-of-phase signal, the ANC system requires a specific algorithm, usually run on a Digital Signal Processing (DSP) unit. Applications of ANC systems cover a wide range of markets, from industry or vehicle interiors to consumer products, such as headphones. In this paper, a structural ANC system applied to a cogeneration plant is investigated, making use of electro-dynamic shakers, accelerometers, and a microphone. The algorithm employed for generating the cancelling signal is a filtered-X Normalized Least Mean Square (FxNLMS). First, measurements of primary and secondary paths performed on the cogeneration plant are presented. Then, the off-line theoretical cancellation performance is evaluated, based on the signals' coherence. An off-line implementation of the FxNLMS algorithm was developed and processed in several configurations, from single reference, single-input, single-output (SISO) to multiple reference, single-input, multiple-output (SIMO). Eventually, a real-time laboratory test was performed with the hardware-in-the-loop technique. The designed architecture demonstrated remarkable performance, with a noise reduction up to 4 dB(A) in the frequency range 50 Hz – 250 Hz.**

Keywords—active noise control, cogeneration plant, electrodynamic shaker, filtered-X LMS, primary path, secondary path, vibration control

I. Introduction

The problem of environmental noise is becoming increasingly serious with the capillary diffusion of industrial plants, transportation, and infrastructures. In solving acoustic noise related problems, traditional passive techniques [1], [2] such as enclosures, barriers, and silencers, are relatively large, costly, and ineffective at low frequencies. For this reason, the use of Active Noise Control (ANC) techniques is more and more common, providing better results at low frequencies with potential benefits in size, weight, volume, and cost. The areas of application for ANC systems are multiple and include automotive [3], appliances, industry, and transportation.

ANC systems [4]–[6] make use of electromechanical or electroacoustic devices to reduce the primary noise by exploiting the principle of destructing interference. The system generates an anti-noise with equal amplitude and opposite phase, which will be summed to the primary source so that both noises cancel each other. In 1936, Lueg [7] proposed the first design of acoustic ANC utilizing a microphone and an electronically driven loudspeaker to generate a cancelling sound. One of the main problems related to this technique is that frequencies, amplitude, phase, and sound velocity of the undesired noise are nonstationary since the characteristics of the acoustic noise source and the environment are time varying. In order to compensate these changes, ANC systems use adaptive filters [8]–[10], which adjust their coefficients to minimize an error signal and can be realized as finite impulse response (FIR), infinite impulse response (IIR), lattice, and transform-domain filters.

ANC can be based on feedforward control [11], if a coherent reference noise input is sensed before it propagates to the receiver, or feedback control [12] where there is no reference input. Moreover, feedforward control can be classified in 1) broadband adaptive feedforward control with a reference sensor, and 2) narrow-band adaptive feedforward control [13], [14] with a reference sensor that is not influenced by the control field (e.g., tachometer). The latter are mainly used with periodic noise sources such as: engines, compressors, motors, fans, and propellers. Other types of algorithms are frequency domain [15], adaptive genetic [16], deep learning-based [17], and single-channel adaptive feedback [18]. A complete analysis of the traditional algorithms can be found in [19].

This work deals with a broadband adaptive feedforward ANC. In these systems, the reference noise input is usually picked up by an accelerometer or a microphone, and then processed to produce the control signal to drive a loudspeaker or an actuator. The most effective approach for this type of system is represented by the Filtered-x Least Mean Square (FxLMS) algorithm, independently derived by Widrow [20] and Burgess [21]. Other variations of the FxLMS algorithm are the Leaky FxLMS algorithm [4], and the FxLMS with feedback neutralization [22].

This work was financed by AB Impianti Srl, to which the University of Parma is grateful.

979-8-3503-1104-4/23/©2023 IEEE

All the ANC systems previously described can be extended from a single channel to a multichannel version [23]–[26]. Instead of a single reference, error, and control signals (usually denoted as 1-1-1 configuration), matrices of signals are used. The multichannel adaptations are generally used in higher complexity applications, such as noise control inside automobile cockpits [27], [28], and propeller-induced noise control inside aircrafts [29].

In this paper, the use of a broadband adaptive feedforward system with normalized FxLMS algorithm is presented to reduce the noise generated by a cogeneration (combined heat and power) plant. First, primary path measurements were taken on the cogenerator with three reference accelerometers and an error microphone, to determine the maximum theoretical cancellation based on primary signals coherence. Then, secondary path measurements were performed between three electrodynamic shakers and the error microphone to evaluate the cancellation by means of the FxLMS algorithm, with an off-line processing. Eventually, the cancellation effect was evaluated with a hardware-in-the-loop technique, making use of a sound card and a Digital Signal Processing (DSP) unit for real-time processing of the FxLMS algorithm. A significant noise reduction was obtained with both off-line and real-time processing, with a cancellation up to 4 dB(A) in the frequency range 50 Hz – 250 Hz, by employing multiple references, single error, multiple output configuration, namely 2-1-2. Such a result was in perfect agreement with the theoretical evaluation.

The paper is organized as follows: Section II describes the experimental measurements of the primary and secondary paths, Section III provides the theoretical evaluation of cancellation performance, while Section IV presents the results obtained with the FxLMS algorithm. Section V, eventually, summarizes the conclusions.

II. Experimental Characterization

Two kinds of measurements are required for the implementation of an ANC system, namely the primary and the secondary paths. The primary path describes the transfer function between the J reference transducers and the M error ransducers, while the secondary path between the K control devices and the M error transducers.

A. Primary path measurement

The measurement configuration scheme is shown in Fig. 1. The cogenerator engine is enclosed in a sheet metal shelter (box in the right part of the figure, with dimensions), on which three (J = 3) PCB Piezotronics accelerometers, single-axis type 333B30 (sensitivity 100 mV/g, +/-50 g bottom scale), have been attached on the long side. A single (M = 1) Bruel&Kjaer (B&K) microphone type 4189 (sensitivity 50 mV/Pa) was placed in front of the structure, varying the distance between 10, 20 and 40 meters.

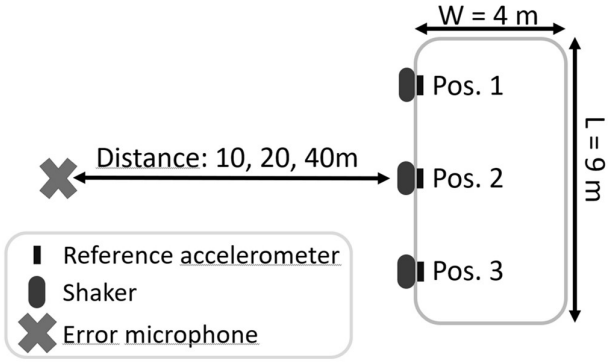

Fig. 1: Primary and secondary paths measurement scheme on the cogenerator.

For each distance, the four signals from the microphone and the accelerometers have been recorded simultaneously using a ZOOM F8 sound card at a sample rate of 48 kHz, for 120 seconds, using the noise emitted by the plant as the signal source.

The Sound Pressure Level (SPL) spectra of the recorded noise at 10, 20 and 40 m can be seen in Fig. 2, in the frequency range 50 Hz – 250 Hz, that is the range in which a significant noise reduction can be achieved, as shown furtherly. The spectra are calculated by averaging multiple Fast Fourier Transform (FFT) blocks, having a $FFT_{size} = 2^{14}$ samples each, overlapped by 75% with a Hann windowing. Hence, the frequency resolution is $df \cong 2.9\ Hz$, calculated as: $df = fs/FFT_{size}$. One can note a reduction of 6 dB every doubling of the distance in the frequency range 55 Hz – 80 Hz, while the energy of the main tonal components (75 Hz, 87.5 Hz, 100 Hz, 112.5 Hz, 125 Hz, and 137.5 Hz) is dependent on the position. Above 145 Hz most of the energy is dissipated already at 40 m distance.

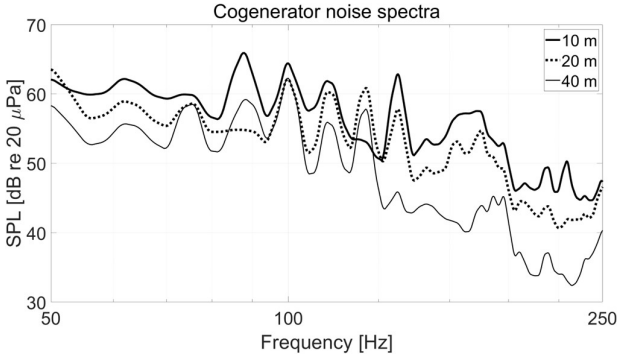

Fig. 2: Spectra of the cogenerator noise measured at 10, 20, and 40 meters. FFT parameters: 2^{14} samples size, Hann windowing, 75% overlap, resolution ~2.9 Hz.

The spectra of acceleration level recorded on the surface of the cogenerator shelter can be seen in Fig. 3, in the frequency range 50 Hz – 250 Hz. One can note that each of the three accelerometers senses most of the tonal components, despite those in positions one and three appear to be the most sensitive.

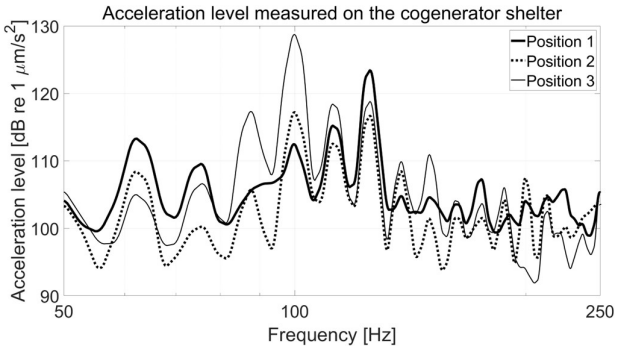

Fig. 3: Spectra of the acceleration level measured on the cogenerator shelter. FFT parameters: 2^{14} samples size, Hann windowing, 75% overlap, resolution ~2.9 Hz.

B. Secondary Path measurement

The secondary path measurements were performed in a similar configuration as in Fig. 1, but three shakers (K = 3) were used at the same positions of the accelerometers, attached to the cogenerator with magnetic bases. The employed shaker is a Monacor type AR-50, having a power rating of 30 Wrms and an 8 Ω impedance. A four channels power amplifier was used, type KS-DR3004 by JVC, having a rated power of 60 Wrms/ch at 4 Ω with 1% of Total Harmonic Distortion (THD). The measurements were performed with the plant turned off, at the three distances of 10, 20 and 40 m, with one shaker at a time. The exponential sine sweep (ESS) technique [30] was employed to get the time domain Impulse Response (IR) between each shaker and the error microphone.

The shaker was excited with an ESS signal of 20 s length in the frequency range 20 Hz – 20 kHz at an output voltage of 10 Vrms, measured under load at the amplifier terminals with a true-RMS tester. Then, the recorded signals were convolved with the inverse ESS, obtaining the IRs between the shakers and the B&K microphone. The ESS allows for separating the linear response, which we are interested in, and the high order harmonic distortion components. Hence, the linear part of the IRs were cut and windowed, as shown in Fig. 4. One can note that the delay occurring between the zero sample and the main peak of the linear IR corresponds to the travel path of the sound wave in air, calculated as:

$$d = \frac{D}{fs} \cdot c_0 \tag{1}$$

where D is the delay in samples, fs is sampling frequency and c_0 is the sound speed. In the case of Fig. 4, the values D = 5600, fs = 48 kHz, and c_0 = 343 m/s provide a result of d = 40 m, as expected.

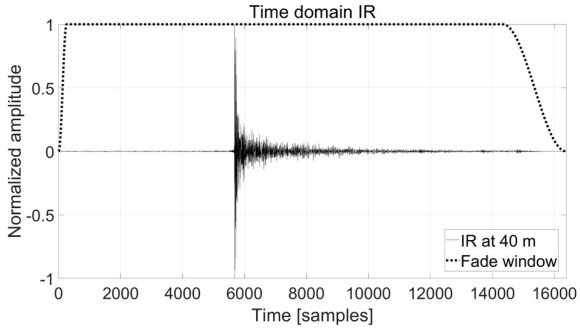

Fig. 4: Time domain IR at 40 m distance.

The secondary path spectra are shown in Fig. 5, for the three positions of the shaker at 40 m distance (see Fig. 1 for the measurement scheme), with the cogenerator noise spectrum superimposed. One can note shakers in positions two and three are particularly effective.

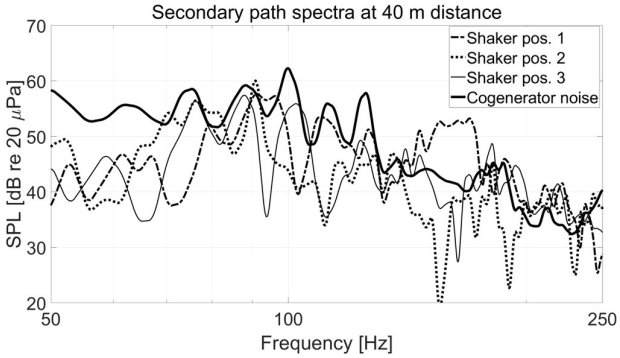

Fig. 5: Spectra of the secondary paths and cogenerator noise at 40 m distance. FFT parameters: 2^{14} samples size, Hann windowing, 75% overlap, resolution ~2.9 Hz.

III. Theoretical Noise Reduction

A. Single-reference, single-input

In this first case of study, only one accelerometer signal is considered at a time as reference. First, the transfer function H_1 between the reference signal x and the error microphone y is calculated in frequency domain, as:

$$H_1(f) = \frac{P_{yx}(f)}{P_{xx}(f)} \tag{2}$$

where f denotes frequency, P_{yx} is the Cross Power Spectral Density (CPSD) between the input signal x and the output signal y, and P_{xx} is the Power Spectral Density (PSD) of the input signal x. Then, H_1 is converted back to a time domain IR, h, through the Inverse Fast Fourier Transform (IFFT). Since the cancellation acts only on the coherent part of noise [4], keeping the incoherent part unchanged, the convolution between the reference signal x and the transfer function h is calculated as:

$$x * h = y' \tag{3}$$

where $*$ denotes the convolution and y' is the part of the noise measured at the error microphone y that is coherent with the reference signal x. Summing the polarity-inverted coherent part $-y'$ with the error microphone signal y, a theoretical cancellation is performed, and the residual noise e is obtained:

$$y + (-y') = e \tag{4}$$

The signals were pre-filtered with a pass-band filter in the range 50 Hz - 250 Hz, i.e., the range of frequencies within ANC systems are mostly effective. The lower limit is practical: effective cancellation at ultra-low frequencies requires heavy and bulky subwoofers or shakers. On the other hand, at higher frequencies the coherence between primary signals is gradually diminishing, making the cancellation ineffective.

The amount of theoretical cancellation for each position of the accelerometers can be seen in Table I, calculated as the difference in terms of SPL before and after cancellation, in dB(A). Only the 40 m distance case is reported, since this is

the case that provided the most significant results, with an SPL reduction up to 4.5 dB(A). This is explained by the fact that the sound wave propagating from the cogenerator plant, at 40 m distance, is more like a plane wave with a slow varying phase.

TABLE I. THEORETICAL NOISE REDUCTION IN THE FREQUENCY RANGE 50 HZ – 250 HZ

Reference accelerometer	SPL reduction at 40 m [dB(A)]
Position 1	4.0
Position 2	4.4
Position 3	**4.5**

B. Multi-reference, single-input

For the evaluation of the combined effect of multiple reference signals to achieve the cancellation at the error microphone, a multi-reference, single-input algorithm has been used. First, the cross-correlation function between the reference signals is calculated:

$$C_{xy}(f) = \frac{|P_{xy}(f)|^2}{P_{xx}(f) \cdot P_{yy}(f)} \qquad (5)$$

where P_{xy} is the CPSD and P_{xx} and P_{yy} are the PSD of the signals x and y. The cross-correlation allows to visualize how similar the reference sensors are to each other in a scale from 0 (complete decorrelation) to 1 (complete correlation). To improve the cancellation with a low number of references, a low value of cross-correlation is required, otherwise the contribution of any additional reference over the previous ones would be negligible. The average cross-correlation in the frequency range 50 Hz – 250 Hz is shown in Fig. 6 in a pseudo-color matrix, where white corresponds to 1 and black corresponds to 0. Cross-correlation values are comprised in the range 0.25 – 0.28, except for the diagonal of the matrix that has unitary values, since it consists in the cross-correlation of a reference with itself, which is always one.

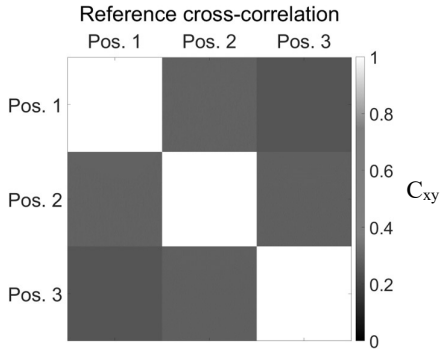

Fig. 6: Cross-correlation matrix of the references averaged in the frequency range 50 Hz – 250 Hz.

To calculate the multi-reference theoretical cancellation, the accelerometer signals are first decorrelated each other. This is performed by solving iteratively eq. (2), (3), and (4) between the *j-th* reference (x) and the remaining J – *j-th* references (y). In this way, a new set of J' uncorrelated reference signals is obtained. Then, the total cancellation is computed by solving iteratively eq. (2), (3), and (4) with the decorrelated references J' as x and with the error microphone signal as y. The noise recorded at the microphone is introduced as the error signal at the first iteration, then at each subsequent iteration the residual noise of the previous one is employed as the new error signal.

The cancellation effect can be seen in the spectra of Fig. 7, where the multi-reference case is compared with the best single-reference case (position 3). One can note the highest amount of noise reduction is obtained on the peaks of the signal, since the system is mainly tonal being the main source an internal combustion engine, with a reduction up to 9.8 dB(A) and 11.0 dB(A) on the tones at 100 Hz and 125 Hz, respectively. The multi-reference approach allowed to increase the noise reduction of about 2 dB(A) on the tonal components and of about 5 dB(A) in the frequency range 100 Hz – 180 Hz. Being a theoretical calculation, no noise additions are detected over the entire frequency range. The average noise reduction in the range 50 Hz – 250 Hz increased from 4.5 dB(A) obtained with the single-reference calculation (position 3) to 5.2 dB(A) obtained with the multi-reference approach, which is a remarkable result.

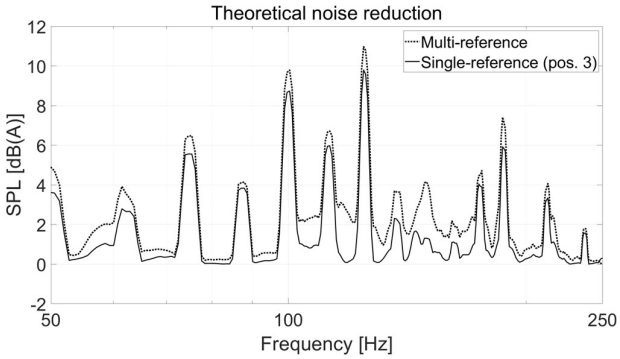

Fig. 7: Theoretical noise reduction, comparison of multi-reference (dot line) and single-reference (solid line). FFT parameters: size of 2^{14} samples, Hann windowing, 75% overlap, resolution ~2.9 Hz.

IV. FILTERED-X LMS ALGORITHM

A block diagram of the Filtered-X Least Mean Square algorithm can be seen in Fig. 8, where P(z) and S(z) are the primary and secondary paths, respectively, and W(z) is the adaptive filter.

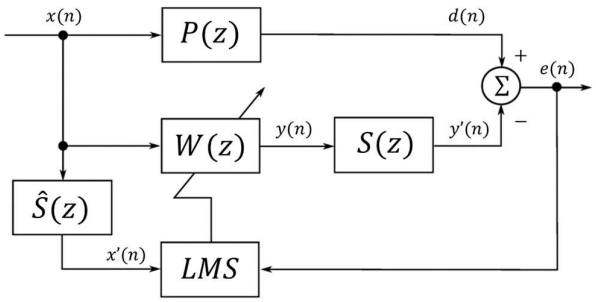

Fig. 8: Block diagram of a FxLMS algorithm.

The residual signal e is expressed as:

$$e(n) = d(n) - s(n) * [w^T(n)x(n)] \qquad (6)$$

where n is the time index, $d(n)$ is the primary disturbance, $s(n)$ is the IR of the secondary path $S(z)$, $*$ denotes the linear convolution, the apex ^{T} denotes the transpose, $w(n) = [w_0(n)\ w_1(n)\ \dots\ w_{L-1}(n)]^T$ are the coefficients of $W(z)$, $x(n) = [x(n)\ x(n-1)\ \dots\ x(n-L+1)]^T$ are the input signal vectors, where L is the filter order. The adaptive filter minimizes the instantaneous squared error $\hat{\xi} = e^2(n)$ using

the steepest descent algorithm, which updates the coefficient vector in the negative gradient direction:

$$w(n+1) = w(n) + \mu x'(n) e(n) \qquad (7)$$

where μ is the step size, $x'(n) = \hat{s}(n) * x(n)$, and $\hat{s}(n)$ is the estimation of $s(n)$. The estimation of the secondary path $\hat{s}(n)$ is usually performed during an initial training stage for most ANC applications.

The coefficient μ must be tuned for each application. This is usually performed manually, balancing the effectiveness and convergence speed of the algorithm (high value of the step size) with the instability of the ANC system. Since a disturbance in the reference signal could lead to instability, the most common method is to use the normalized FxLMS algorithm, in which the step size is adjusted by weighting it proportionally to the reference signal power, as:

$$\mu = \frac{\beta}{x'^{T}(n) x'(n)} \qquad (8)$$

where β is a constant between 0 and 2.

A. Off-line implementation

First, the FxNLMS algorithm was tested with different configurations in an off-line implementation (MATLAB development environment). Several cases have been studied, exploiting various combinations of references (J = 1, 2, 3) and shakers (K = 1, 2, 3), from a basic single-reference, Single-Input Single-Output (SISO) and going to the more complex multi-reference, Single-Input Multi-Output (SIMO). With the aim of reducing the computation time, all the signals (references, error, and secondary path IRs) were down sampled by a factor 16, thus reducing the sampling frequency from 48 kHz to 3 kHz, which is still 12 times the maximum interested frequency, that is 250 Hz. A number of samples equal to W = 256 were used for the adaptive filter, while the step size μ was iteratively adjusted to maximize the noise reduction.

The optimal results for each configuration are shown in Table II, in terms of SPL reduction in dB(A) averaged in the frequency range 50 Hz – 250 Hz. Also in this case, the performance of the system provided the highest cancellation amount with the error microphone positioned at 40 m distance from the cogenerator. One can note the most significative result is obtained in a multi-reference SIMO configuration with J = 2 references and K = 2 shakers, respectively located in positions (2;3) and (1;2). An overall cancellation amount of 4.0 dB(A) was obtained, with a limited improvement of 0.4 dB(A) over the single-reference SISO case.

TABLE II. NOISE REDUCTION WITH FXNLMS ALGORITHM IN THE FREQUENCY RANGE 50 HZ – 250 HZ

	Accelerometer position	**Shaker position**	**SPL reduction at 40 m [dB(A)]**
J=1; M=1; K=1	2	2	3.6
J=1; M=1; K=2	2	1 ; 2	3.8
J=2; M=1; K=1	2 ; 3	2	3.8
J=2; M=1; K=2	**2 ; 3**	**1 ; 2**	**4.0**

The spectrum of the multi-reference SIMO cancellation is shown in Fig. 9, in comparison with the multi-reference theoretical result. The tonal components are mostly cancelled up to 140 Hz, while a reduction of performance is observed at higher frequencies and in the cancellation of the non-tonal part of the signal in the range 100 Hz – 180 Hz, where the multi-reference theoretical algorithm is instead quite effective. A few broadband noise additions are detected, however not exceeding 1 dB(A).

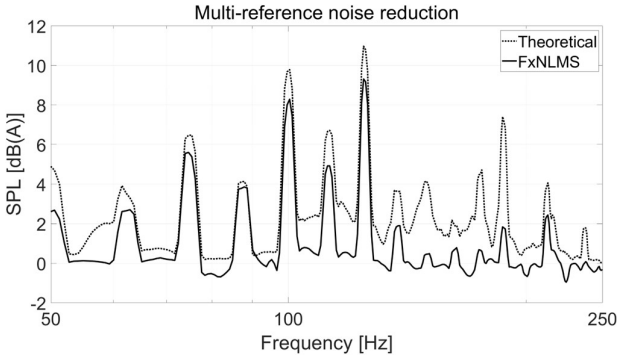

Fig. 9: Multi-reference noise reduction, comparison of theoretical (dot line) and SIMO FxNLMS (solid line). FFT parameters: size of 2^{14} samples, Hann windowing, 75% overlap, resolution ~2.9 Hz.

B. Real-time hardware-in-the-loop

A real-time laboratory test of the system was performed by exploiting the hardware-in-the-loop technique and a DSP unit, namely ADAU1466Z by Analog Devices. It features four input channels and eight output channels and can be programmed to run an LMS algorithm via Sigma Studio®.

The hardware-in-the-loop configuration can be seen in Fig. 10. A computer is connected to a soundcard (ZOOM F8) to send and receive digital signals. Analog signals are delivered from the output of the soundcard to the input channels of the DSP. Then, the processed signals are delivered from the analog output of the DSP to the input channels of the soundcard, and back to the computer.

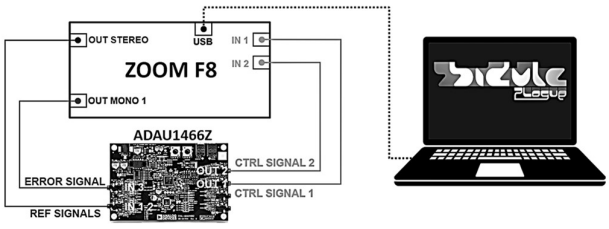

Fig. 10: Hardware-in-the-loop configuration for real-time test of the ANC system.

The software employed is Plogue Bidule, a real-time audio processor, which allows for low-latency processing of digital signals through Virtual Studio Technology (VST) plug-ins and internal DSP modules. The schematic of Plogue Bidule processing can be seen in Fig. 11. The computer delivers the reference and the error signals to the soundcard. The ADAU1466Z processes them through a FxLMS algorithm, obtaining the control signals, which are sent back to the computer through the soundcard. Control signals are convolved with the secondary path IRs and then summed with the recorded noise of the cogenerator, obtaining the error signal.

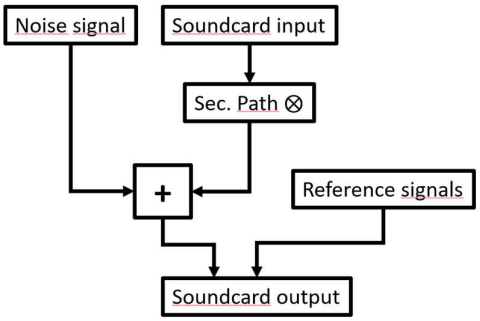

Fig. 11: Real-time signal processing in Plogue Bidule software.

The FxLSM block was configured with a filter length of W = 256 samples and a step size $\mu = 0.1$. Also in this case, both references and error signals were down sampled by a factor 16 to reduce the computational effort on the DSP. Then, the control signals were up sampled by the same factor to return at the starting sample rate of 48 kHz. Both down-sampling and up-sampling were performed by the DSP unit, while Plogue Bidule always operating at 48 kHz.

The error signal was recorded during the real-time operation of the system, and it is shown in the time domain in Fig. 12. Initially the FxLMS algorithm is switched off, then it is switched on and the error starts to reduce. The noise reduction stabilizes after the complete convergence of the system is reached ("ANC conv." in the figure). The convergence time was about 7 s for this case.

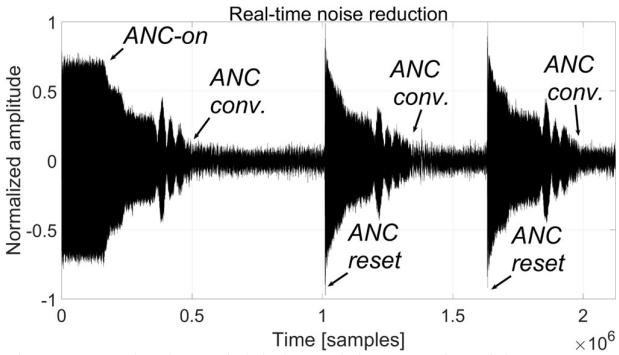

Fig. 12: Error signal recorded during real-time operation of the M-FxLMS algorithm in the hardware-in-the-loop test.

The results obtained with the real-time hardware-in-the-loop processing were identical to those obtained with the off-line processing already shown in Table II, thus confirming the validity of the employed method.

V. Conclusion

An effective application of a vibro-acoustical Active Noise Control system was presented, which aims at reducing the noise generated by a cogeneration plant using electro-dynamic shakers, accelerometers, and a microphone.

First, experimental measurements of primary and secondary paths performed on the cogeneration plant were presented. Then, the cancellation performance was theoretically evaluated with a single-reference and a multi-reference approach. An off-line implementation of a FxLMS algorithm was developed, and the definition of the working principles was given too. Several algorithm configurations have been evaluated, starting with a single-reference, single-input, single-output scheme, and ending up with a multiple-reference, single-input, multiple-output scheme. The cancellation performance, evaluated in terms of SPL reduction in dB(A), was in line with the theoretical prediction. Eventually, a real-time test of the cancelling system with the hardware-in-the-loop technique was presented. It provided the same results of the off-line implementation, thus confirming the effectiveness of the method.

This work proven that a significative noise reduction of a cogeneration plant noise can be achieved with a FxLMS algorithm, in both an off-line processing stage and real-time implementation. A cancellation amount of 4.0 dB(A) in the 50 Hz – 250 Hz frequency range was obtained with a multi-reference SIMO configuration.

References

[1] C. M. Harris, *Handbook of acoustical measurements and noise control*. McGraw-Hill New York, 1991.

[2] L. L. Beranek and I. L. Ver, "Engineering sound and vibration control. Principles and applications." Wiley Interscience, New York, 1992.

[3] C. Belicchi *et al.*, "ANC: A Low-Cost Implementation Perspective," in *SAE Technical Papers*, 2022. doi: 10.4271/2022-01-0967.

[4] S. M. Kuo and D. R. Morgan, *Active noise control systems*, vol. 4. Wiley, New York, 1996.

[5] P. A. Nelson and S. J. Elliott, *Active control of sound*. Academic press, 1991.

[6] C. C. Fuller, S. J. Elliott, and P. A. Nelson, *Active control of vibration*. Academic press, 1996.

[7] P. Lueg, "UNITED STATES PATENT OFFICE 2,043,416 PROCESS OF SILENCING SOUND OSCLEATONS."

[8] G. C. Goodwin and K. S. Sin, *Adaptive filtering prediction and control*. Courier Corporation, 2014.

[9] S. D. Stearns, "of Aldapfive Signal Processing," 1985.

[10] S. Haykin and B. Widrow, "Least-Mean-Square Adaptive Filters," 2003.

[11] S. M. Kuo and J. Tsai, "Acoustical mechanisms and performance of various active duct noise control systems," *Applied Acoustics*, vol. 41, no. 1, pp. 81–91, 1994.

[12] H. F. Olson and E. G. May, "Electronic sound absorber," *J Acoust Soc Am*, vol. 25, no. 6, pp. 1130–1136, 1953.

[13] B. Chaplin, "The cancellation of repetitive noise and vibration," in *INTER-NOISE and NOISE-CON Congress and Conference Proceedings*, 1980, pp. 699–702.

[14] E. Ziegler Jr, "Selective active cancellation system for repetitive phenomena." Google Patents, Oct. 1989.

[15] E. R. Ferrara, C. F. N. Cowan, and P. M. Grant, "Frequency-domain adaptive filtering," *Adaptive filters*, vol. 145, 1985.

[16] C.-Y. Chang and D.-R. Chen, "Active Noise Cancellation Without Secondary Path Identification by Using an Adaptive Genetic Algorithm," *IEEE Trans Instrum Meas*, vol. 59, no. 9, pp. 2315–2327, 2010, doi: 10.1109/TIM.2009.2036410.

[17] H. Zhang and D. Wang, "Deep MCANC: A deep learning approach to multi-channel active noise control," *Neural Networks*, vol. 158, pp. 318–327, 2023.

[18] P. A. Nelson and S. J. Elliott, *Active control of sound*. Academic press, 1991.

[19] S. M. Kuo and D. R. Morgan, "Active noise control: a tutorial review," *Proceedings of the IEEE*, vol. 87, no. 6, pp. 943–975, May 1999, doi: 10.1109/5.763310.

[20] B. Widrow, D. Shur, and S. Shaffer, "On adaptive inverse control," *Fifteenth asilomar conference on circuits, systems and computers*, pp. 185–189, 1981, Accessed: May 29, 2023. [Online]. Available: https://isl.stanford.edu/~widrow/papers/c1981onadaptive.pdf

[21] J. C. Burgess, "Active adaptive sound control in a duct: A computer simulation," *J Acoust Soc Am*, vol. 70, no. 3, pp. 715–726, 1981.

[22] L. Poole, G. Warnaka, and R. Cutter, "The implementation of digital filters using a modified Widrow-Hoff algorithm for the adaptive cancellation of acoustic noise," in *ICASSP'84. IEEE International Conference on Acoustics, Speech, and Signal Processing*, 1984, pp. 215–218.

[23] S. S. Popovich, D. E. Melton, and M. C. Allie, “New adaptive mulit-channel control systems for sound and vibration,” in *INTER-NOISE and NOISE-CON Congress and Conference Proceedings*, 1992, pp. 405–408.

[24] S. M. Kuo and B. M. Finn, “A general multi-channel filtered LMS algorithm for 3-D active noise control systems,” *Second Int. Con. on Recent Developments in Air and Structure Borne Sound and Vibration, Auburn AL*, pp. 345–352, 1992.

[25] Z. Luo, D. Shi, J. Ji, and W. Gan, “Implementation of Multi-channel Active Noise Control based on Back-propagation Mechanism.” 2022.

[26] V. Patel and N. V George, “Multi-channel spline adaptive filters for non-linear active noise control,” *Applied Acoustics*, vol. 161, p. 107142, 2020.

[27] C. F. Ross, “The control of noise inside passenger vehicles,” in *Proc. Recent Advances in Active Control of Sound Vibration*, 1991, pp. 671–681.

[28] P. N. Samarasinghe, W. Zhang, and T. D. Abhayapala, “Recent Advances in Active Noise Control Inside Automobile Cabins: Toward quieter cars,” *IEEE Signal Process Mag*, vol. 33, no. 6, pp. 61–73, 2016, doi: 10.1109/MSP.2016.2601942.

[29] S. J. Elliot, P. A. Nelson, I. M. Stothers, and C. C. Boucher, “In-flight experiments on the active control of propeller-induced cabin noise,” *J Sound Vib*, vol. 140, no. 2, pp. 219–238, 1990.

[30] A. Farina, “Simultaneous measurement of impulse response and distortion with a swept-sine technique,” in *Audio engineering society convention 108*, 2000.